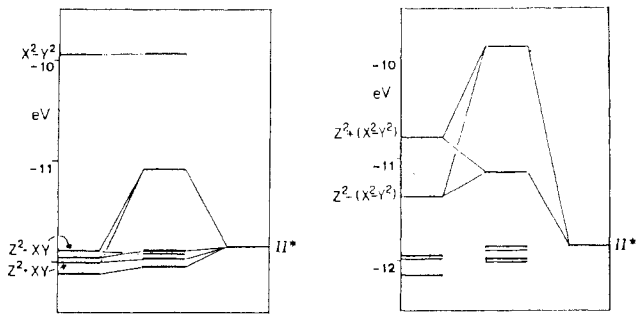

Figure 8. Extended Hückel molecular orbital diagrams: (a) Mn(hfac)$_2$(NITPh)$_2$; (b) Mn(hfac)$_2$(NITMe)$_2$.

where i represents magnetic orbitals that are essentially the d orbitals of the metal and r is the π^* magnetic orbital of the radical. Each individual $J_{i,r}$ constant has both a ferro- and an antiferromagnetic component. Since the energies of the z^2, xz, and yz orbitals of the square-planar fragment, which overlap significantly with the radical π^* orbital, are not too different from each other, we may use the sum of the squared overlap, $\sum S_{i,r}^2$, as a criterion for estimating the relative variation of J in the series.

In Figure 7 we plot $S = \sum S_{i,r}^2$ vs the angular parameters. When the Mn–O distance is shortened, the overlaps increase, making more intense both the ferro- and antiferromagnetic components. The parameter ϕ has substantially little effect on the sum of the squared overlaps. When θ is increased, the overlap increases, except for small values of ψ, whereas S actually decreases when θ is increased. Therefore, we may expect that the antiferromagnetic coupling increases when both θ and ψ are increased; indeed, if we compare the data reported in Table VIII for Mn(hfac)$_2$(TEMPO)$_2$ and Mn(hfac)$_2$(PROXYL)$_2$, we see that the latter has both θ and ψ larger than the former and a larger coupling constant. Therefore, these results seem to be encouraging us to continue in the analysis.

In order to have closer approximations to the true molecules and to attempt to rationalize the experimental results for all the Mn(hfac)$_2$(radical)$_2$ adducts thus far reported, we performed sample calculations by using fragments A–D shown in the Experimental Section. The values of the calculated S for the models of Mn(hfac)$_2$(TEMPO)$_2$ and Mn(hfac)$_2$(PROXYL)$_2$ are in the same order as the experimental J values, confirming the results suggested above, as shown in Table VIII.

If we compare Mn(hfac)$_2$(NITPh)$_2$ with Mn(hfac)$_2$(TEMPO)$_2$ and Mn(hfac)$_2$(PROXYL)$_2$, we see that the value of S for the first is intermediate between those of the other two and also that the exchange coupling constant is intermediate between the other two; therefore, it seems, notwithstanding the difference in the nature of the radicals, that S can be used as a good indicator of the extent of antiferromagnetic coupling. On the other hand since the geometrical parameters for Mn(hfac)$_2$(PROXYL)$_2$ and Mn(hfac)$_2$(NITPh)$_2$ are very similar, it must be concluded that the smaller overlap in the NITPh derivative is due to the delocalized structure of the ligand, suggesting that the coupling of nitronyl nitroxides may be weaker than that of nitroxides.

Comparing Mn(hfac)$_2$(NITPh)$_2$ with the cis adduct Mn(hfac)$_2$(NITMe)$_2$, we see that also in this case the order of S corresponds to the order of the coupling constants, although in this case the difference in the J values is rather small. In all the above discussion we have neglected the ferromagnetic component of J. It must not be identically zero, otherwise the spins would be coupled to give only a populated quartet ground state. However the satisfactory predictions reached by using only the antiferromagnetic component show that the role of the ferromagnetic component is still a minor one in the series of complexes we considered.

Acknowledgment. The financial support of the Italian Ministry of Public Education and the CNR is gratefully acknowledged.

Registry No. Mn(hfac)$_2$(NITPh)$_2$, 113533-12-3; Mn(hfac)$_2$(NITMe)$_2$, 113567-52-5; Mn(hfac)$_2$, 19648-86-3.

Supplementary Material Available: Anisotropic thermal parameters for the non-hydrogen atoms of Mn(hfac)$_2$(NITPh)$_2$ (Table SI), anisotropic thermal parameters for the non-hydrogen atoms of Mn(hfac)$_2$(NITMe)$_2$ (Table SII), complete listings of bond distances and angles for I (Tables SIV and SV) and II (Tables SVI and SVII), χT values for I and for II (Table SVIII), and parameters used in extended Hückel calculations (Table SIX) (20 pages); observed and calculated structure factors for I (Table SIII) and II (Table SX) (26 pages). Ordering information is given on any current masthead page.

(22) Eremin, M. V.; Rakitin, Yu. V. *Phys. Status Solidi B* **1977**, *80*, 579. Eremin, M. V.; Rakitin, Yu. V. *Phys. Status Solidi B* **1977**, *82*, 221.

Contribution from the Departments of Chemistry, University of Trondheim, Trondheim, Norway, The University of Reading, Whiteknights, Reading, Berkshire RG6 2AD, U.K., and Queen Mary College, The University of London, London, U.K.

Gas-Phase Electron Diffraction Study of Tetrakis(dimethylamido)zirconium(IV), Zr(NMe$_2$)$_4$

Kolbjørn Hagen,[1a] Catherine J. Holwill,[1b] David A. Rice,*[,1b] and Jonathan D. Runnacles[1c]

Received November 18, 1987

The molecular structure of Zr(NMe$_2$)$_4$ has been studied by gas-phase electron diffraction. The experimental data are fitted by a model that contains planar C$_2$N–Zr fragments bound to a ZrN$_4$ core that has a T_d symmetry. Small deviations from T_d symmetry cannot be excluded, but the deviation of the ∠N–Zr–N angle from the T_d value must be less than 5°. The lowest R factors were obtained with the ZrN$_4$ fragment having D_{2d} symmetry and with ∠N(1)–Zr–N(2) = 107.4 (48)°, but the difference from the tetrahedral model is not statistically significant. Two different values for the C(1)–N(1)–Zr–N(2) torsion angle (∠Φ_2) [109.7 (87)° and 127.7 (66)°] gave minima in the least-squares refinements with ∠Φ_2 = 109.7 (87)°, giving a slightly lower R factor, but the difference from that obtained with ∠Φ_2 = 127.7 (66)° was not statistically significant. The values, with estimates of uncertainties (2σ) for the principal distances (r_g) and angles ($\angle_\alpha$), are r(Zr–N(1)) = 2.071 (11) Å, r(C(1)–N(1)) = 1.461 (4) Å, r(C(1)–H(1)) = 1.118 (12) Å, ∠C(1)–N(1)–C(1^1) = 111.2 (11)°, and ∠N(1)–C(1)–H(1) = 108.7 (30)°, with ∠N(1)–Zr–N(2) being assumed as 109.47°.

Introduction

Tetrakis(dimethylamido) complexes, M(NMe$_2$)$_4$, have been isolated for a number of transition elements,[2] and thus they provide one of the few classes of compounds where it could be possible to determine the effect of d^n configuration upon structure. Examination of the metal–nitrogen stretching modes has led to the suggestion that the MN$_4$ fragment in a number of these M-

(1) (a) The University of Trondheim. (b) The University of Reading. (c) The University of London.

(2) Bradley, D. C. *Adv. Inorg. Chem. Radiochem.* **1972**, *15*, 259.

0020-1669/88/1327-2032$01.50/0

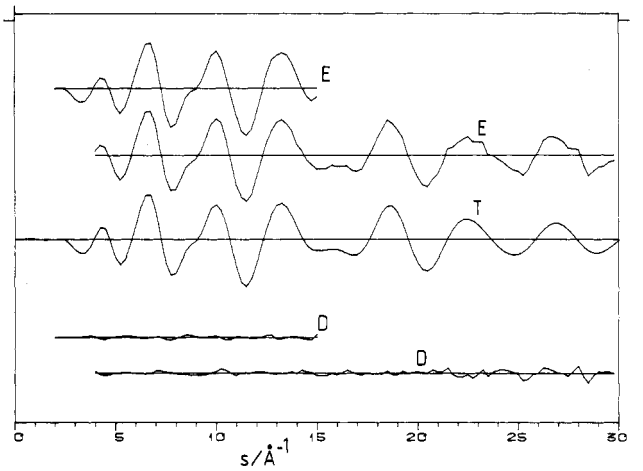

Figure 1. Intensity curves $sI_m(s)$ for $Zr(NMe_2)_4$. Experimental curves (E) are averages of all plates for the two camera distances. The theoretical curve (T) was calculated from the structural parameters shown in Table I for model 1, which has a ZrN_4 core of T_d symmetry. The difference curves (D) result from the subtracting the relevant part of the theory curve from the experimental curves.

$(NMe_2)_4$ compounds deviates from T_d symmetry.[3] The deviations are likely to be small and so may be masked by crystal packing effects in the solid, and it has proved difficult in many instances to obtain crystals suitable for single-crystal X-ray studies. Accordingly we decided to use gas-phase electron diffraction, where any lattice effects are removed, to study the structures of a number of dialkylamides having the formula $M(NMe_2)_4$. We chose to commence our investigation by examining the d^0 compound $Zr(NMe_2)_4$.

Two related structural studies have been reported. The structure of $Mo(NMe_2)_4$ has been determined by X-ray methods[4] while an electron diffraction investigation of $Sn(NMe_2)_4$ has been made.[5]

Experimental Section

Preparation of $Zr(NMe_2)_4$. In a Schlenk tube, $Zr(NMe_2)_4$ was prepared by allowing $ZrCl_4$ to react with $LiNMe_2$ according to published procedures.[6] The product was purified by sublimation and samples (approximately 1 g) were placed in sealed ampules that could be loaded directly into the Balzers Eldigraph KDG-2 apparatus at the University of Oslo[7,8] and opened in situ.

Data were obtained at nozzle-to-plate distances of 497.95 and 248.12 mm with nozzle temperatures of 80–90 °C. The electron wavelength was calibrated against diffraction pictures of benzene.[9] Four plates from the short and three from the long camera distance experiments were used in the final analysis. The data cover the ranges $2.00 \le s \le 15.00$ Å^{-1} and $4.00 \le s \le 30.00$ Å^{-1} at intervals of $\Delta s = 0.25s$. The experimental data were processed as previously described[10-14] with scattering factors taken from ref 15 and 16. Average curves were produced for each camera distance, and these are depicted in Figure 1. The reduced intensity data and the background curve data are available as supplementary material.

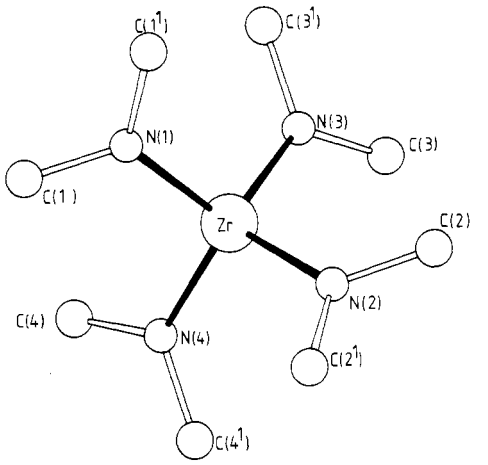

Figure 2. Atom-numbering scheme used in the study of $Zr(NMe_2)_4$. The hydrogen atoms are numbered according to the carbon atom to which they are bound; thus bound to C(1) are H(1), H(1¹), and H(1²).

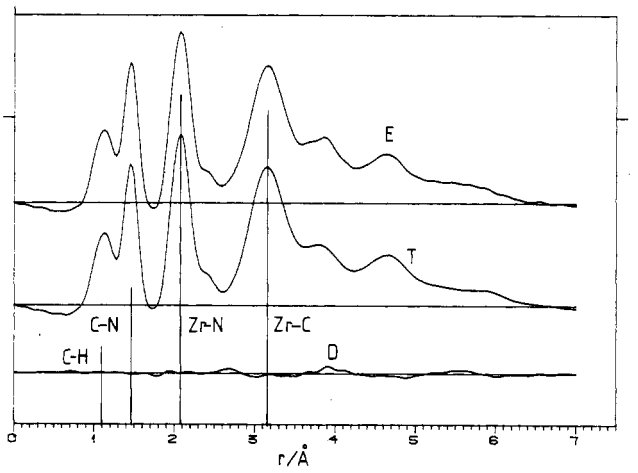

Figure 3. Radial distribution curves for $Zr(NMe_2)_4$ showing experimental (E), theoretical (T), and difference (D) curves. The curves were calculated from the curves in Figure 1 after multiplications by $Z_{Zr}Z_N/f_{Zr}f_N \exp(-0.0025s^2)$ and from theoretical data for the unobserved area $s < 2.0$ Å^{-1}. The vertical lines indicate the position of selected interatomic distances, height being proportional to weight of distance. However, many of the peaks in the radial distribution curve contain contributions from more than one interaction.

Analysis of the Structure

The molecule is depicted in Figure 2, which contains the atom-numbering scheme. The methyl groups were assumed to have local C_{3v} symmetry with the threefold axis coinciding with the C–N bonds. A model was chosen with eight independent parameters, three bond distances [r(C(1)–H(1)), r(C(1)–N(1)), r(Zr–N(1))], three valence angles [$\angle$N(1)–Zr–N(2), $\angle$C(1)–N(1)–C(1¹), $\angle$N(1)–C(1)–H(1)], and two torsion angles $\angle\Phi_1$ = H(1)–C(1)–N(1)–Zr [the H atoms are numbered according to the C atom to which they are bound; thus, those bound to C(1) are H(1), H(1¹) and H(1²)] and $\angle\Phi_2$ = C(1)–N(1)–Zr–N(2). The model was designed to allow the ZrN_4 fragment to deviate from T_d symmetry and attain D_{2d} symmetry with $\angle$N(1)–Zr–N(2) being the angle that occurs twice in such a fragment. With $\angle$N(1)–Zr–N(2) fixed at 109.47°, the ZrN_4 moiety of the molecule has T_d symmetry and thus all the $\angle$N–Zr–N angles are equal.

Root-mean-square vibrational amplitudes (l), perpendicular amplitude corrections (K), and centrifugal distortion constants (δr) were calculated from an assumed valence force field by using values for the force constants obtained from studies of related molecules.

Refinements of the structure were carried out by the least-squares procedure method[17] based on the intensity curves by adjusting one theoretical curve to the two average experimental curves (one from each of the two nozzle-to-plate distances) using a unit weight matrix. Some of the vibrational amplitudes were refined together with the geometrical

(3) Bradley, D. C.; Gitlitz, M. J. *J. Chem. Soc. A* **1969**, 980.
(4) Chisholm, M. H.; Cotton, F. A.; Extine, M. W. *Inorg. Chem.* **1978**, *17*, 1329.
(5) Vilkov, L. V.; Tarasenko, N. A.; Prokofev, A. K. *Zh. Strukt. Khim.* **1970**, *11*, 129.
(6) Bradley, D. C.; Thomas, I. M. *J. Chem. Soc.* **1960**, 3857.
(7) Zeil, W.; Haase, J.; Wegmann, L. *Z. Instrumentenkd.* **1966**, *74*, 84.
(8) Bastiansen, O.; Graber, R.; Wegmann, L. *Balzers High Vacuum Rep.* **1969**, *25*, 1.
(9) Tamagawa, K.; Iijima, T.; Kimura, M. *J. Mol. Struct.* **1976**, *30*, 243.
(10) Hagen, K.; Hedberg, K. *J. Am Chem. Soc.* **1973**, *95*, 1003.
(11) Gundersen, G.; Hedberg, K. *J. Chem. Phys.* **1969**, *51*, 2500.
(12) Andersen, B.; Seip, H. M.; Strand, T. G.; Stølevik, R. *Acta Chem. Scand.* **1969**, *23*, 3224.
(13) Hagen, K.; Hobson, R. J.; Holwill, C. J.; Rice, D. A. *Inorg. Chem.* **1986**, *25*, 3659.
(14) Hedberg, L. *Abstracts of Papers*, 5th Austin Symposium on Gas-Phase Molecular Structure, Austin, TX, Mar 1974; p 37.
(15) *International Tables for X-ray Crystallography*; Kynoch: Birmingham, U.K., 1974.
(16) Sellers, H. L.; Schafer, L.; Bonham, R. A. *J. Mol. Struct.* **1978**, *49*, 125.
(17) Hedberg, K.; Iwasaki, M. *Acta Crystallogr.* **1964**, *17*, 529.

Table I. Final Structural Parameters for $Zr(NMe_2)_4$[a]

param	model 1[b] $r_g/\angle_\alpha$	l_{calcd}	$l_{refined}$	model 2[b] $r_g/\angle_\alpha$
r(Zr–N(1))	2.071 (11)	0.061	0.069 (8)	2.071 (11)
r(C(1)–N(1))	1.461 (4)	0.047	0.048 (5)	1.461 (4)
r(C(1)–H(1))	1.118 (12)	0.079	0.094 (10)	1.117 (12)
∠N(1)–Zr–N(2)	[109.47]			107.4 (48)
∠C(1)–N(1)–C(1[1])	111.2 (11)			111.3 (12)
∠N(1)–C(1)–H(1)	108.7 (30)			108.6 (32)
$\angle\Phi_1$[c]	[0.0]			[0.0]
$\angle\Phi_2$[d]	109.7 (89)			111.2 (93)
Selected Dependent Parameters				
∠N(1)–Zr–N(3)	[109.47]			110.5 (25)
∠Zr–N(1)–C(1)	124.4 (5)			124.3 (6)
r(Zr···C)	3.124 (10)	0.167	0.162 (8)	
r(C(1)···C(1[1]))	2.407 (16)	0.088	0.069 (13)	
r(N(1)···N(2))	3.371 (13)	0.156	0.186 (37)	
r(N(1)···H(1))	2.097 (37)	0.108		
r(C(2)···N(1))	4.414 (53)	0.207		
r(C(2[1])···N(1))	4.047 (55)	0.256		
r(C(3)···N(1))	4.737 (18)	0.150		
r(C(3[1])···N(1))	3.659 (18)	0.283		
r(C(4)···N(1))	3.866 (50)	0.261		
r(C(4[1])···N(1))	4.570 (41)	0.181		
r(C(1)···C(2))	4.746 (34)	0.341		
r(C(1)···C(2[1]))	4.792 (153)	0.324		
r(C(1[1])···C(2))	5.621 (90)	0.217		
r(C(1[1])···C(2[1]))	4.746 (34)	0.341		
r(C(1)···C(3))	5.221 (74)	0.272		
r(C(1)···C(3[1]))	3.774 (43)	0.393		
r(C(1[1])···C(3))	5.924 (45)	0.179		
r(C(1[1])···C(3[1]))	4.789 (52)	0.320		
r(C(1)···C(4))	5.221 (74)	0.272		
r(C(1)···C(4[1]))	5.924 (45)	0.179		
r(C(1[1])···C(4))	3.774 (43)	0.393		
r(C(1[1])···C(4[1]))	4.789 (52)	0.320		
r(Zr···H)[e]	3.817 (18)	0.181		
r(Zr···H)[e]	3.017 (34)	0.235		

[a] Distances (r_g) and amplitudes (l) in ångstroms and angles ($\angle_\alpha$) in degrees. Parenthesized uncertainties are 2σ and include estimates of systematic errors and correlation in the experimental data. Values in square brackets were kept constant in the least-squares refinement. [b] In model 1 the ZrN_4 moiety was assumed to be tetrahedral whereas in model 2 it was assigned D_{2d} symmetry. [c] $\angle\Phi_1$ is the H(1)–C(1)–N(1)–Zr torsion angle. [d] $\angle\Phi_2$ is the C(1)–N(1)–Zr–N(2) torsion angle. [e] With $\angle\Phi_1$ set at 0.0° there are two Zr···H distances, the one with the H atoms out of the Zr–N–C plane having a multiplicity twice that of the distance with the H atom in the plane.

parameters; the rest were kept constant at the calculated values. In the early stages of the study a model was adopted that allowed for a nonplanar geometry around the nitrogen atoms. However, the best agreement was obtained with a planar or very nearly planar geometry, and in all subsequent refinements such planarity was assumed. Different values were tested for the H(1)–C(1)–N(1)–Zr torsion angle ($\angle\Phi_1$) and the best agreement was obtained with $\angle\Phi_1 = 0°$ and so in all the later refinements $\angle\Phi_1$ was kept constant at 0°.

Variation of the C(1)–N(1)–Zr–N(2) torsion angle ($\angle\Phi_2$) indicated minima in the agreement factor R for two different values of $\angle\Phi_2$. A variety of starting values were tested for $\angle\Phi_2$, and depending upon the starting value, the refinements converged with values of $\angle\Phi_2$ of either ≈110 or ≈128°. However the difference in between the two refinements was not statistically significant.

Refinement of ∠N(1)–Zr–N(2) indicated that no significant improvement of the fit to the data was obtained by using a ZrN_4 fragment with D_{2d} symmetry over that obtained with T_d symmetry although the R factor was slightly better with a ZrN_4 fragment of D_{2d} symmetry. All the other parameters were nearly independent of small changes in ∠N(1)–Zr–N(2).

The radial distribution (RD) curves were calculated in the usual manner by Fourier transformation of the $s(I_m(s))$ values after multiplication by $(Z_{Zr}Z_N/f_{Zr}f_N)\exp(-0.0025s^2)$. In Figure 3 are depicted the experimental and theoretical RD curves and the difference curve. The theoretical curve was calculated for a species with a T_d ZrN_4 fragment, and the values for the parameters are given in Table I for a T_d model. The calculated curves for model with a D_{2d} ZrN_4 core could not be distinguished from that shown. The results of the final refinments for the T_d and D_{2d} models are given in Table I, and Table II contains the correlation matrix for the model having a T_d core.

Discussion

The results of our structural investigation of $Zr(NMe_2)_4$ are consistent with the presence in the molecule of a ZrN_4 moiety with T_d symmetry or with small deviations from this symmetry. The lowest R factor was obtained with a D_{2d} ZrN_4 fragment in which the angle that occurs twice in such a fragment deviated slightly from the T_d value. However, the difference in the angle from the tetrahedral value was not significant, especially as the model with lower symmetry has an extra parameter to be adjusted in the least-squares refinement and so would be expected to give a lower R factor. Thus the results of our electron diffraction study cannot decide if the symmetry of the ZrN_4 moiety deviates slightly from T_d to D_{2d}, but our test refinements do show that in a D_{2d} model ∠N(1)–Zr–N(2) must be within 5° of the tetrahedral value. All the refinements indicate the presence of a planar or very nearly planar C_2N–Zr group. The same planarity was also observed in $Mo(NMe_4)_4$.[4] The amplitude l(Zr···C) refined to a large value [0.162 (8) Å], and this could indicate a small nitrogen out-of-plane force constant especially as l(C···C) has a "normal" value of 0.069 (13) Å, and l(Zr···C) and l(C···C) are not highly correlated (Table II).

As described earlier, two different values for the rotation about the N–Zr bonds were found to produce minima in the least squares refinements. A value of 90° for the ∠C(1)–N(1)–Zr–N(2) torsion angle corresponds to a rigorously D_{2d} symmetry for the $Zr(NC_2)_4$ fragment of the molecule. The model was designed so that the rotation of all four C_2N groups when viewed along the N–Zr bond occurred in an identical manner. The values obtained for $\angle\Phi_2$, even though they carry large uncertainties do indicate that in $Zr(NMe_2)_4$ the $Zr(NC_2)_4$ fragment deviates markedly from D_{2d} symmetry [$\angle\Phi_2 = 109.7\ (87)°$ in the final model]. In the solid state $Mo(NMe_2)_4$[4] was found to be D_{2d} as all the C–N–Mo–N torsion angles were found, within the limits of experimental error, to be 90°. The molybdenum compound forms triclinic crystals so there is no crystallographic reason for it to show D_{2d} symmetry. Thus the difference between the two structures is obviously a manifestation of the importance of intramolecular forces in Zr-

Table II. Correlation Matrix (×100) for the Parameters in $Zr(NMe_2)_4$

param	σ_{LS}[a]	r_1	r_2	r_3	$\angle_4$	$\angle_5$	$\angle_6$	l_7	l_8	l_9	l_{10}	l_{11}	l_{12}
r(Zr–N)	0.0034	100	−7	−3	1	−88	8	1	4	33	6	−22	23
r(C–N)	0.0008		100	13	−22	−2	3	13	3	12	16	5	22
r(C–H)	0.0029			100	−5	−12	0	−3	2	5	3	−1	3
∠C–N–C	0.36				100	12	−11	1	2	23	−37	−16	−54
∠N–C–H	1.00					100	−7	−1	−5	−35	−7	12	−23
$\angle\Phi_2$[b]	2.91						100	−1	−5	−5	3	0	6
l(C–H)	0.0026							100	18	13	12	−3	5
l(C–N)	0.0011								100	45	26	−6	9
l(Zr–N)	0.0027									100	19	−23	5
l(Zr···C)	0.0040										100	2	61
l(C···C)	0.0042											100	0
l(N···N)	0.0182												100

[a] Standard deviations from the least-squares refinement. Distances (r) and amplitudes (l) in angstroms and angles in degrees. [b] $\angle\Phi_2$ = C(1)–N(1)–Zr–N(2) torsion angle.

$(NMe_2)_4$ and intermolecular interactions in solid $Mo(NMe_2)_4$.

The planarity around the nitrogen atoms is caused by the N to Zr p_π to d_π donation, which reduces the Lewis acidity of the metal. Therefore the Zr-N bonds have some multiple bond character that is not changed by rotation of the C_2-N groups around the N-Zr bonds as the ZrN_4 group retains its D_{2d} or higher T_d symmetry irrespective of the value of ∠C(1)-N(1)-Zr-N(2) torsion angle.

The results do not give an unambiguous geometry for the ZrN_4 fragment. In $Sn(NMe_2)_4$ a tetrahedral geometry was assumed for the co-ordination sphere of the tin atom,[5] while in $Mo(NMe_2)_4$, the N-Mo-N angles covered the range 107.3 (2)-112.5 (2)° with the average being 109.5 (1.9)°. If nonbonded d electrons exert any steric effect, the MoN_4 fragment is more likely than the ZrN_4 fragment to exhibit D_{2d} symmetry. This is because in $Mo(NMe_2)_4$ the two d electrons occupy the nonbonding $d_{x^2-y^2}$ orbital that is in the xy plane which bisects the four equivalent N-Mo-N angles of the D_{2d} fragment. It may be, as stated in the introduction, that this effect is masked in the solid state for $Mo(NMe_2)_4$.

It would appear from our study that the covalent radius of Zr (1.45 Å) is so large that it readily allows deformation of the ZrN_4 moiety, deviation of the ∠C(1)-N(1)-Zr-N(2) torsion angle from 90°, and out of plane bending of the C_2-N fragments. It would therefore be interesting to determine the structures of $Ti(NMe_2)_4$ and $V(NMe_2)_4$, where the metal atoms have smaller covalent radii [r_{Ti} = 1.32 Å and r_V = 1.22 Å] than zirconium and vanadium has a d^1 configuration. The difference between the covalent radii of titanium and zirconium is known to have a profound influence upon structure. For example at room temperature titanium(IV) chloride consists of monomeric tetrahedral molecules while zirconium(IV) has a chain structure with octahedrally coordinated metal centers. Some differences between $Ti(NMe_2)_4$ and $Zr(NMe_2)_4$ attributable to changes in covalent radius have been reported. Measurements on benzene solutions have shown that while $Ti(NMe_2)_4$ is monomeric, $Zr(NMe_2)_4$ exists as a monomer-dimer equilibrium.[3,6] We thus believe that a more rigid gas-phase structure is to be expected for $Ti(NMe_2)_4$ than is reported here for the zirconium analogue.

The metal-nitrogen distance in $Zr(NMe_2)_4$ [2.071 (11) Å] is as expected slightly longer than that observed in $Mo(NMe_2)_4$ [1.926 (6) Å],[4] while that in $Sn(NMe_2)_4$ is 2.045 (7) Å.[5] The values obtained for r(C(1)-N(1)) [1.461 (4) Å], r(C(1)-H(1)) [1.118 (12) Å], ∠C(1)-N(1)-C(1[1]) [111.2 (11)°], and ∠N(1)-C(1)-H(1) [108.7 (30)°] are in accord with related data previously determined by electron diffraction.[5,18,19]

Acknowledgment. We thank Professor D. C. Bradley of Queen Mary College, London, for his interest in this work. We are grateful to Snefrid Gundersen and Hans Volden of the University of Oslo for their technical help. We thank SERC for financial support (C.J.H. and J.D.R.) and NATO for the award of a travel grant, No. 117/82.

Registry No. $Zr(NMe_2)_4$, 19756-04-8.

Supplementary Material Available: Tables of reduced intensity data and background curve data (4 pages). Ordering information is given on any current masthead page.

(18) Clark, A. H.; Anderson, G. A. *J. Chem. Soc. D* **1969**, 1082.
(19) Vilkov, L. V.; Tarasenko, N. A. *J. Chem. Soc. D* **1969**, 1176.

Contribution from the Institute of Inorganic Chemistry, Westfaelische Wilhelms-Universitaet, 4400 Muenster, Federal Republic of Germany

A Series of Tris(μ-fluoro)divanadates(III, IV, V) Containing the Bioctahedral $[V_2(O,F)_9]^{3-}$ Unit. Synthesis, Characterization, and Structures of $(NMe_4)_3V_2F_9$, $(NMe_4)_3V_2O_2F_7$, $(NMe_4)_3V_2O_4F_5$, and $(NMe_4)_2KV_2O_4F_5 \cdot H_2O$

Norbert Buchholz, Manfred Leimkühler, Leonidas Kiriazis, and Rainer Mattes*

Received November 23, 1987

Tetramethylammonium salts of the anions $[V_2O_4F_5]^{3-}$, $[V_2O_2F_7]^{3-}$, and $[V_2F_9]^{3-}$, each consisting of face-sharing double octahedra, have been prepared and their structural chemistries investigated. $(NMe_4)_3V_2O_4F_5$, $(NMe_4)_3V_2O_2F_7$, and $(NMe_4)_3V_2F_9$ crystallize in the hexagonal $Cs_3Cr_2Cl_9$ type structure, space group $P6_3/m$, with $Z = 2$. $(NMe_4)_3V_2O_4F_5$: a = 8.076 (4) Å, c = 18.703 (8) Å. $(NMe_4)_3V_2O_2F_7$: a = 8.031 (5) Å, c = 18.571 (7) Å. $(NMe_4)_3V_2F_9$: a = 8.050 (9) Å, c = 18.671 (11) Å. With use of 647, 591, and 477 unique data ($I \geq 1.96\sigma(I)$), the three structures were refined to R = 0.044, 0.055, and 0.055, respectively. In $[V_2O_4F_5]^{3-}$ and $[V_2O_2F_7]^{3-}$ the oxo ligands are bonded terminally. Both anions are disordered in the solid state to adopt the symmetry of the space group. The vanadium-vanadium distances decrease with oxidation state in the order $[V_2O_4F_5]^{3-}$, $[V_2O_2F_7]^{3-}$, $[V_2F_9]^{3-}$ from 3.138 (1) and 2.977 (2) to 2.894 (3) Å. The V-F (bridging) distances decrease in the same order from 2.114 (2) and 2.071 (3) to 2.044 (3) Å. The repulsion between the metal atoms is diminished by these ligands, which have very short nonbonding contacts. $(NMe_4)_2KV_2O_4F_5 \cdot H_2O$ crystallizes in orthorhombic space group $Pnma$ with a = 10.724 (2) Å, b = 18.796 (4) Å, c = 8.658 (2) Å, and $Z = 4$. The structure was refined to R = 0.036 with use of 1485 unique data. The dimensions of the $[V_2O_4F_5]^{3-}$ ion here and in $(NMe_4)_3V_2O_4F_5$ are very similar. The magnetic moment of $(NMe_4)_3V_2F_9$ at room temperature is 2.65 μ_B per vanadium.

Introduction

Compounds containing the binuclear anion $[M_2X_9]^{3-}$ (X = Cl, Br, I) are well-known.[1] Recently oxo compounds like $Ba_3M_2O_9$ (M = Te(VI),[2] W(VI)[3]) and oxo fluoro compounds like $Cs_3Mo_2O_6F_3$,[4] $Cs_3V_2O_4F_5$,[5,6] and $Cs_3V_2O_2F_7$[5-7] containing face-sharing bioctahedral units have been characterized. The $A_3M_2X_9$ compounds crystallize in three types of structures that consist of hexagonal AX_3 layers but have different stacking modes and

(1) (a) Chabot, B.; Parthe, E. *Acta Crystallogr., Sect. B: Struct. Crystallogr. Cryst. Chem.* **1978**, *B34*, 645. (b) Leuenberger, B.; Briat, B.; Canit, J. C.; Furrer, A.; Fischer, P.; Güdel, H. U. *Inorg. Chem.* **1986**, *25*, 2930. (c) Stranger, R.; Grey, I. E.; Madson, I. C.; Smith, P. W. *J. Solid State Chem.* **1987**, *69*, 162.
(2) Jacobson, A. J.; Scanlon, J. C.; Poeppelmeier, K. R.; Longo, J. M. *Mater. Res. Bull.* **1981**, *16*, 359.
(3) (a) Kemmler-Sack, S.; Treiber, U. *Z. Anorg. Allg. Chem.* **1979**, *455*, 65. (b) Poeppelmeier, K. R.; Jacobson, A. J.; Longo, J. M. *Mater. Res. Bull.* **1980**, *15*, 339.
(4) Mattes, R.; Mennemann, K.; Jäckel, N.; Rieskamp, H.; Brockmeyer, H. J. *J. Less-Common Met.* **1980**, *76*, 199.
(5) Mattes, R.; Förster, H. *J. Less-Common Met.* **1982**, *87*, 227.
(6) Wall, F.; Pausewang, G.; Babel, D. *J. Less-Common Met.* **1971**, *25*, 257.
(7) Waltersson, K. *Cryst. Struct. Cryst. Struct. Commun.* **1978**, *7*, 507.

0020-1669/88/1327-2035$01.50/0